

A Mixed Integer Approach for Obtaining Unique Solutions in Source Inversion of Water Networks¹

Carl D. Laird, Lorenz T. Biegler²

Department of Chemical Engineering, Carnegie Mellon University, Pittsburgh, PA, 15213, USA

Bart G. van Bloemen Waanders

Sandia National Laboratories³, Albuquerque, NM, 87109, USA

Keywords: Water distribution systems; Water security; Optimization, mixed-integer; Water contamination;

Abstract

This paper addresses the problem of contamination source determination in municipal drinking water networks. In previous work, the authors introduced a large scale nonlinear programming approach for identifying both the time and location of contamination sources given concentration information from a limited number of sensors. Due to the sparseness of the sensor grid, this problem inherently has non-unique solutions. The problem was therefore regularized and the regularized solution provided an approximate linear combination of the possible injection scenarios. In this paper, a mixed integer quadratic program is presented to refine the solution provided by the nonlinear programming formulation. We introduce a two-phase approach. In the *n-phase*, the number of likely injection locations is estimated. Using this information, the *e-phase* is performed to extract the likely injection scenarios from the family of non-unique solutions. This two-phase approach is tested on a realistic municipal water network model with approximately 400 nodes, simulating 5 different injection scenarios. In all 5 examples, the approach was able to determine the correct number of injection locations and identify a set of possible injection scenarios containing the actual simulated injections.

¹Financial support for this work was provided by the National Science Foundation under ITR Grant ACI-021667.

²Corresponding author, email: lb01@andrew.cmu.edu

³Sandia is a multiprogram laboratory operated by Sandia Corporation, a Lockheed-Martin Company, for the United States Department of Energy under Contract DE-AC04-94AL85000.

Introduction

Presidential Decision Directive 63 identified water systems as one of the critical infrastructures to the United States. Following this directive and the passing of *The Public Health, Security, and Bioterrorism Preparedness and Response Act* there has been increased research effort in both assessing the vulnerability of drinking water systems and proposing protection measures. Drinking water networks are vulnerable to chemical and biological contamination and while physical security is being used to limit access to some potential contamination locations, the distribution system itself remains largely unprotected. One proposed method of protection is the installation of an early warning detection system. Sensors installed at various locations throughout the drinking water network could provide warning in the event of a contamination.

On its own, an early warning detection system (Ostfeld and Salomons, 2003; Berry et al., 2003), provides only a coarse measure of the time and location of the contamination event. In previous work (Laird et al., 2005, 2004; van Bloemen Waanders et al., 2003) the authors introduced a large scale nonlinear programming approach that used real-time concentration information from an installed sensor grid to determine accurately the time and location of the contamination event. This approach introduced unknown, time dependent injection terms at every node in the network and formulated a quadratic program to solve for the time profiles of these injection terms. The complete, time discretized water quality model was included as explicit constraints in the least squares estimation problem, giving a large scale quadratic program (QP). The formulation for this problem included the following assumptions:

- Installed sensors are capable of providing concentration measurements of the contaminant or, at least some linear measure of the degree of contamination. These measurements need not be perfect, but they are assumed to be normally distributed about the true value.
- Network flowrates are known, either from simulations, flow measurements, or some combined estimation procedure.

Injection from different nodes could be indistinguishable given the measurements from the sparse sensor grid, causing the QP to have non-unique solutions. Regularizing the problem forced a unique solution to the QP that was an approximate linear combination of distinct non-unique solutions. This results in a single solution that contains a family of possible injection scenarios. Unfortunately, from this solution alone, it can be difficult to determine the likely number of injections and the distinct injection scenarios that give rise to the linear combination. Furthermore, due to modeling and measurement error, the solution may include injection profiles that have only a minor effect on reducing the least squares error.

In this paper, we build on the results of Laird et al. (2005) and add a discrete capability in order to determine the likely number of contamination events and the distinct scenarios that are truly influential in reducing the least squares error. We reformulate the large scale NLP problem from Laird et al. (2005) into a mixed integer quadratic programming (MIQP) formulation. While the size of this full MIQP is prohibitive, considering only the space of solutions provided by the original NLP greatly reduces the size of the MIQP and allows the use of standard mixed integer solvers in a real-time context. A two-phase approach is proposed. First, an *n-phase* is used to identify the likely number of contamination events occurring in the network (the number of injection locations). Then, given the number of events, an exploration phase, or *e-phase* identifies the distinct injection scenarios that give rise to the solution of the original NLP.

The *Background* section gives a brief description of the formulation presented in Laird et al. (2005), followed by a discussion of solution non-uniqueness and the regularized problem. Following that, we introduce the mixed integer formulation and show how the problem size can be reduced using active-set information from the original NLP. Then, the two-phase approach is introduced and a formal description of the algorithm is given. Finally, the effectiveness of this approach is demonstrated on a realistic municipal water network model in the section, *Results*. Five different contamination scenarios are tested with both single and multiple injection locations. The results demonstrate that the approach is very effective at correctly determining the number of contamination events

and likely injection scenarios that correspond to the observed concentrations.

Background

The purpose of the work in Laird et al. (2005) was to present a formulation for solving the inverse problem of identifying the time and location of contaminant injections in real-time, using concentration information from sensors installed at a limited number of nodes. This work assumed that contaminations could occur from any network node and introduced unknown, time dependent contaminant injections at each node in the network. As with water quality simulation techniques (Shang et al., 2002; Zierolf et al., 1998; Rossman and Boulos, 1996), this approach used network flows as known inputs and modeled the water quality only. The optimization problem was then written as a weighted least squares minimization of the errors between the calculated and measured concentrations subject to the partial differential constraints of the water quality model. This infinite dimensional optimization problem was discretized in time, using an origin tracking algorithm to remove the need to discretize in space, and a large scale quadratic program was formulated from the discretized model. Due to the non-uniqueness of solutions, regularization was applied to the formulation.

Using Θ to refer to the set of discretizations in time, and \mathcal{P} and \mathcal{N} to refer to the complete set of network pipes and nodes, respectively, the original continuous quadratic program (OCQP) for the inversion problem can be formulated as (Laird et al., 2005),

$$\min_{\bar{c}, c, m} f = \frac{1}{2} [c - c^*]^T W [c - c^*] + \frac{\rho}{2} m^T m \quad (1)$$

$$\text{s.t.} \quad \bar{c} - Pc = 0, \quad (2)$$

$$\bar{N}\bar{c} + Nc + Mm = 0, \quad (3)$$

$$m \geq 0, \quad (4)$$

where $\bar{c} = [\dots \bar{c}_{ij}^I, \bar{c}_{ij}^O \dots]$, $\forall i \in \mathcal{P}, j \in \Theta$ is a vector of pipe concentrations for the inlet (\mathcal{I}) and outlet (\mathcal{O}) of every pipe, discretized in time, $c = [\dots c_{ij} \dots]$, $\forall i \in \mathcal{N}, j \in \Theta$ is the vector of calculated concentrations for every node at every time discretization, and $m = [\dots m_{ij} \dots]$, $\forall i \in \mathcal{N}, j \in \Theta$ is the vector of unknown contaminant mass injections

for every node at every time discretization. The matrix P is defined by the origin tracking algorithm, and the matrices \bar{N} , N , and M are the Jacobians of the discretized mass balance constraints (for junctions and storage tanks) with respect to the pipe concentrations, node concentrations, and unknown injections, respectively. The function f is a regularized weighted least squares objective where c^* are the measured concentrations and the diagonal matrix W is a flow-based weighting matrix for the least squares errors, with nonzero elements only for sensor nodes at sample times.

The second term in the objective is a regularization term that forces a unique solution to the problem. First, consider the unregularized case. With $\rho=0$, problem (1-4) is a convex, but not necessarily strictly convex, QP; therefore, the QP solution is a global minimum for the objective value, but the minimizer it is not necessarily unique. This non-uniqueness is due to the limited number of sensors.

Consider the grid network shown in Figure 1 with sensors installed at every second node (indicated by the grey shading) and a single reservoir water source at node 26. Network flows are constant in the directions indicated by the arrows with demands at the boundary nodes only. These demands were selected to introduce symmetry about an axis through nodes 1 and 26 and pipe travel times that range from 0.5 to 5 hours. Selecting node 13 as the injection location, we introduce contaminant from time, $t = 0.5$ to $t = 1$ hours. With the flows used in this network, the contaminant will flow from node 13 to nodes 12 and 8 in about an hour and a half, where the sensors will then detect the contaminant. If we consider only the observed concentration measurements at nodes 8 and 12 (and zero concentration measurements from the other sensors), we realize that there are two distinct injection scenarios capable of producing the observed concentrations. The contaminant could have been injected at node 13 (the actual injection) or at both nodes 8 and 12 simultaneously. Since any linear combination of these two scenarios is also a possible solution, there are an infinite number of solutions to the unregularized problem. With a small positive value for ρ , however, the QP obtains a unique *regularized* solution. The regularization term balances the contribution from the non-unique solutions, giving a single solution that is an approximate linear

combination of distinct injection scenarios. The value of ρ used is small relative to the magnitude of the least squares term and does not dramatically alter the optimal objective value.

Laird et al. (2005) demonstrate the source inversion capability on the grid network example described above. Simulating the injection from node 13 with EPANET (Rossman, 2000) and using the origin tracking algorithm to describe the pipe time delays, the authors formulate problem (1-4) with $\rho=1 \cdot 10^{-4}$, 5 minute timesteps, and a time horizon of 4 hours (48 timesteps) and the solution is shown in Figure 2. This figure shows the time profiles for the non-zero mass injections only with time in hours along the abscissa and the mass flowrate of the injections along the ordinate. As expected, we see that nodes 8, 12, and 13 all contribute injection profiles to the solution. The effect of regularization is apparent. The solution given is an approximate linear combination of the two distinct solutions discussed above. With the simplicity of the grid network topology and flow patterns, it is straightforward for us to examine Figures 1 and 2 and infer the two solutions of interest, namely an injection at node 13 at $t = 0.5$ hours, or a simultaneous injection at nodes 8 and 12 at $t = 2$ hours. Unfortunately, for a more complex network, with time varying flow patterns, interpreting these solution profiles is non-trivial.

Refining the solution of the original NLP, we would would like to know the number of likely injections occurring in the network and the possible injection scenarios involving this number of locations. For example, armed with the information that a single injection from node 13 is capable of producing the observed concentrations, we would likely investigate this location first, as opposed to nodes 8 and 12 where injections would need to be timed precisely to coincide with the time delays from node 13.

Mixed Integer Formulation

In this section, we introduce a mixed integer formulation derived from the OCQP. We will first show how the size of the base formulation can be reduced by considering only the space of solutions provided by the OCQP. We will then introduce discrete variables

and formulate a mixed integer quadratic program that allows us to restrict the number of injection locations and add cuts to exclude specific injection scenarios. This will form the basis for our two-phase approach described in the next section.

Consider the grid network problem presented earlier. With 26 nodes and 48 timesteps, this problem has 1248 elements in m (one for each node at each timestep). If we look at the solution of the OCQP given in Figure 2, however, we immediately notice that most of the elements of m are zero at the solution (i.e. most of the bound constraints are active). There are only 18 nonzero elements of m at the solution (6 timesteps for each of the 3 nodes). Furthermore, there are only 3 nodes represented in the solution, 8, 12, and 13. To search within the solution provided by the OCQP, we are only interested in these nonzero elements and the reduced set of node locations. Therefore, if we first solve the OCQP and identify the elements of m that are zero (or below some detection limit), we can remove these variables and formulate the MIQP in the space of the nonzero variables only.

It is first convenient to rewrite the OCQP, problem (1-4), in terms of m only, letting $A = -(\bar{N} \cdot P + N)^{-1}M$,

$$\min_m f = \frac{1}{2} [Am - c^*]^T W [Am - c^*] + \frac{\rho}{2} m^T m \quad (5)$$

$$\text{s.t.} \quad m \geq 0, \quad (6)$$

Let m^* be the solution of the injection variables from the OCQP. We can then partition m into m_0 , the elements that were zero at the solution of the OCQP, and m_+ , the elements that were positive,

$$m = \begin{bmatrix} m_0 & m_+ \end{bmatrix},$$

$$m_0 = \{m_{ij} : m_{ij}^* = 0, \forall i \in \mathcal{N}, j \in \Theta\},$$

$$m_+ = \{m_{ij} : m_{ij}^* > 0, \forall i \in \mathcal{N}, j \in \Theta\}. \quad (7)$$

Let the set $\mathcal{N}_+ = \{i : m_{ij}^* > 0, \forall i \in \mathcal{N}, \forall j \in \Theta\}$ contain all the nodes that are

represented by the solution of the OCQP, that is all the nodes that have at least one nonzero injection at some point in time. Let the set, $(\Theta_+)_i = \{j : m_{ij}^* > 0, \forall j \in \Theta\}$ contain the timesteps that are represented by the solution of the OCQP for node i . With these definitions, m_+ can be equivalently defined as $m_+ = \{m_{ij}, \forall j \in (\Theta_+)_i, \forall i \in \mathcal{N}_+\}$.

Partitioning $A = [A_0 \ A_+]$, we can rewrite problem (5-6) in terms of $[m_0 \ m_+]$. Since the m_0 elements are fixed at zero, they can be removed from the problem,

$$\min_{m_+} f = \frac{1}{2} [A_+ m_+ - c^*]^T W [A_+ m_+ - c^*] + \frac{\rho}{2} m_+^T m_+ \quad (8)$$

$$\text{s.t.} \quad m_+ \geq 0. \quad (9)$$

Since we have only removed the variables that will be zero at the solution of the OCQP, the solution for m_+ from problem (8-9) is the same as that of the OCQP and problem (5-6). Of course, this reformulation can not be used to reduce the size of the OCQP, since it requires that we first evaluate the solution of the full OCQP to determine the active-set. However, if we first solve the OCQP, then identify the zero and nonzero elements of m , we can use problem (8-9) as the basis for formulating the MIQP in terms of the nonzero variables only. This greatly reduces the number of nodes and timesteps to consider in the MIQP.

It is convenient to introduce a new variable $\Delta m = m_+ - m_+^*$, and rewrite the objective (8) as,

$$\begin{aligned} f = & \frac{1}{2} [A_+ m_+^* - c^*]^T W [A_+ m_+^* - c^*] + \frac{\rho}{2} [m_+^*]^T [m_+^*] \\ & + [A_+ \Delta m]^T W [A_+ m_+^* - c^*] + \rho \Delta m^T m_+^* \\ & + \frac{1}{2} [A_+ \Delta m]^T W A_+ \Delta m + \frac{\rho}{2} \Delta m^T \Delta m. \end{aligned} \quad (10)$$

It is clear that the first two terms in equation (10) are constant. From the first order

optimality conditions of problem (5-6), we have that

$$A_+^T W [A_+ m_+^* + A_0 m_0^* - c^*] + \rho m_+^* - v_+^* = 0 \quad (11)$$

$$A_0^T W [A_+ m_+^* + A_0 m_0^* - c^*] + \rho m_0^* - v_0^* = 0, \quad (12)$$

where v are the dual variables for the lower bounds on m . Since m_+ is the set of all variables whose solution values were nonzero (i.e. their bound constraints were not active), from the complementarity conditions we know that $v_+=0$. Furthermore, $m_0=0$ and equation (11) simplifies to $A_+^T W [A_+ m_+^* - c^*] + \rho m_+^* = 0$. Therefore, the third and fourth terms in equation (10) sum to zero and we only consider the final two terms for our objective in the following mixed integer formulation,

$$\min_{\Delta m, y} f_\Delta = \frac{1}{2} \Delta m^T Q \Delta m + \frac{\rho}{2} \Delta m^T \Delta m \quad (13)$$

$$\text{s.t.} \quad Ly_i \leq m_{ij}^* + \Delta m_{ij} \leq Uy_i, \quad \forall i \in \mathcal{N}_+, j \in (\Theta_+)_i \quad (14)$$

$$\sum_{i \in \mathcal{N}_+} y_i = n \quad (15)$$

$$\|y - b^k\|_1 \geq 1, \quad \forall k \in \{1..K\}. \quad (16)$$

We label this formulation BMIQP(n, K), the base mixed integer quadratic program. Since $c=A_+ m_+$, the matrix, $Q=A_+^T W A_+$ can be efficiently calculated by perturbing elements of m_+ and solving the forward model to find the response on c . Here $y_i \in \{0, 1\}$ is a binary variable that allows positive injections for node i only if $y_i=1$. The parameters L and U are reasonable lower and upper bounds on the injection terms and constraint (14) is a standard big-M constraint (Biegler et al., 1997). Constraint (15) allows us to restrict the feasible region to only those solutions involving n injection locations. The parameter n can be any value between zero and $|\mathcal{N}_+|$, where $|\cdot|$ indicates the cardinality of the set. Constraint (16) allows us to add integer cuts (Biegler et al., 1997) eliminating unlikely scenarios or previously visited solutions. K is the number of integer cuts, where the parameter b^k is the vector of binary values for cut k . That is, all $y = b^k, \forall k \in \{1..K\}$,

will be disallowed.

To show the effectiveness of this MIQP formulation and how it may be used, we again consider the grid network example and formulate problem (13-16) using the solution of the OCQP, from Figure 2. Dropping the integer constraints (15-16), we can completely enumerate all the possible combinations for the binary variables.

Table 1 shows all 8 enumerated solutions. We are interested in two pieces of information. First, we want to know the number of likely injection locations. Second, we want to know all the distinct injection scenarios (involving that number of injection locations) that are capable of producing the observed data. Notice that the top entry in the table, Solution 1, tells us immediately that an injection at node 13 alone is able to reproduce the observed data precisely. Furthermore, Solutions 4 and 5 show the objective function is worsened by adding node 8 or node 12 to the solution with node 13. While Solution 2 with nodes 8 and 12 together are also capable of reproducing the data precisely, it is likely that we would first investigate node 13. Furthermore, we see from Solution 6 and 7 that nodes 8 or 12 on their own are not capable of matching the observed data. Any injection from 8 must be accompanied by an injection from 12 and vice-versa. These results confirm what we already know from the network topology and flow conditions, but for a more complex system, these scenarios may not have been easily inferred by the solution of the OCQP alone. The MIQP formulation is able to tell us that we have one likely injection location and that location is node 13.

In this small grid example, we were able to enumerate all the possible integer solutions. For larger examples, however, this may be combinatorially intractable. Instead, we propose a two-phase search procedure.

Two-Phase Approach

Formulation (13-16) forms the base mixed integer quadratic program for our two-phase approach. In the n -phase we first identify the number of likely contamination events. Here, we solve BMIQP($n, 0$) for all $n \in \{1..|\mathcal{N}_+\}$. By examining the value of the objective function, seek the smallest value of n that still indicates a reasonable match

with the observed data. Let $f_{\Delta}^*(n, 0)$ be the optimal objective value for BMIQP($n, 0$). The value of $f_{\Delta}^*(|\mathcal{N}_+|, 0)=0$ is the best match that we can achieve. In defining f_{Δ} , we dropped the first two constants in equation (10), therefore a value of zero does not mean a perfect match with the data, but rather as good a match as the OCQP. The value of $f_{\Delta}^*(0, 0)$ is the value of the objective function if we forced all elements of m to zero (i.e. $f_{\Delta}^*(0, 0) = f_{\Delta}(\Delta m = -m_+^*)$) and provides a reasonable measure for worst case behavior. Using this notation, we introduce the following definition,

$$\sigma(n, K) = 1 - \frac{f_{\Delta}^*(n, K)}{f_{\Delta}^*(0, 0)}. \quad (17)$$

By this definition, a value of $\sigma(n, K) = 1$ means that we have as good a match with the data as possible. A value of $\sigma(n, K) = 0$ indicates that we have essentially no matching of the data. In the n -phase procedure we will search for the smallest value of n that produces a value for $\sigma(n, 0)$ approaching 1 and call this value n^* . This is the smallest number of injection locations that are capable of producing the observed data and this situation will be our first investigation priority. Note that it appears as though this selection of n^* is merely favoring scenarios which involve the fewest injection locations (i.e. the simplest possibility), but actually, the justification is much stronger. If the true injection scenario involved more than n^* injection locations, then the true scenario would need to be precisely timed to appear as though it had originated from fewer locations. This would require detailed, real-time information about the current flow patterns in the network. Consider again the grid network example. It is not merely that an injection at node 13 is a single injection and therefore more likely than injections at nodes 8 and 12. Rather, an injection at node 13 alone is more likely than injections at nodes 8 and 12 that are so precisely timed that they can also look like an injection from node 13 on its own. This would require a coordinated injection and precise knowledge of the delays between the nodes. This type of coordinated scenario is unlikely, however, it is not impossible and the approach does not prevent us from also considering scenarios with more than n^* injection locations.

Once we have identified the likely number of injection locations n^* , we enter the e -

phase or exploratory phase of the search procedure. Here, we seek to identify all the distinct scenarios involving n^* injection locations that provide a reasonable match of the observed concentrations. Let $y^*(n^*, K)$ be the optimal solution for the binary variables from BMIQP(n^*, K). In the *e-phase*, we first solve BMIQP($n^*, K=0$) and record the values of the elements of $y^*(n^*, 0)$, the first possible injection scenario. Using constraint (16), we cut $y^*(n^*, 0)$ from the set of possible solutions, increment K , and solve BMIQP($n^*, K=1$), this time, finding $y^*(n^*, 1)$. Iterating, we obtain a set of possible distinct injection scenarios, stopping the search when the value of $\sigma(n^*, K)$ no longer indicates a match with the observed data. The complete two-phase search algorithm is defined as follows:

Two-Phase Search Algorithm

1. Solve the OCQP
2. Identify the elements of m_+
3. Calculate Q
4. Formulate problem BMIQP(n, K)
5. The *n-phase*; find n^* , the likely number of injection locations:
 - 5.1. For $n = \{1..|\mathcal{N}_+|\}$, solve BMIQP($n, 0$) and record $\sigma(n, 0)$
 - 5.2. Examine the sigma values and select n^*
6. The *e-phase*; find possible distinct injection scenarios with n^* injection locations:
 - 6.1. Let $K = 0$
 - 6.2. Solve BMIQP(n^*, K)
 - 6.3. if $\sigma(n^*, K) < \sigma_{tol}$ or if BMIQP(n^*, K) is infeasible then
 - Stop.
Otherwise,
 - Record $y^*(n^*, K)$ as a possible injection scenario
 - Add the cut, letting $K = K + 1$ and $b^K = y^*(n^*, K)$
 - Goto step 6.2

The parameter, σ_{tol} determines a point to stop the search. In the numerical results for this paper, this value was set to $\sigma_{tol} = 0.8\sigma(n^*, 0)$.

Numerical Results

In this section we will demonstrate the effectiveness of the two-phase approach on a realistic municipal water network model. This model, shown in Figure 3, has 394 junctions, 534 pipes, 1 reservoir, 1 tank, 1 pump, and 4 valves. (The nodes have been morphed from their original locations, but the connectivity remains true.) We select 50 sensor locations by first creating a weighted distribution for the nodes, assigning a value for each of the nodes based on the total flow through the node in a 24 hour period. To ensure that nodes with zero flow are not arbitrarily excluded from selection, all nodes are given a weight of at least 5 percent of the maximum weight. We then randomly draw from this distribution to select the sensor nodes.

The two-phase approach is tested with five examples. There are two examples testing the single injection scenario, one with an injection from node 435, and one with an injection from node 801. There are also two examples testing the double injection scenario, one with injections from nodes 435 and 51, and one with injections from nodes 435 and 801. Finally, we test a triple injection scenario with simultaneous injections from nodes 435, 801, and 51.

For each of these scenarios, the spread of contaminant is simulated using EPANET (Rossman, 2000). We perform a 24 hour simulation with all contaminant injections being a pulse injection from hour 6 to hour 7. The OCQP problem is formulated with a 6 hour time horizon, starting at hour 4 through hour 10. This is equivalent to running the source inversion 4 hours following the true injection time.

In all cases, we formulate the full OCQP using a software tool (Laird et al., 2005) that parses the EPANET input and output files, performs the origin tracking algorithm, and writes the optimization problem in AMPL (Fourer et al., 1993) format. This AMPL problem is then solved with the CPLEX optimization package (www.ilog.com). Using the solution of the OCQP, we find the set m_+ by selecting all elements of m greater than a threshold tolerance. Forward simulations are performed using equations (2-3) for each perturbed element in m_+ . The matrix $Q=A_+^T W A_+$ is then calculated and the base mixed integer quadratic program BMIQP(n, K) is written in AMPL format.

All mixed integer problems were also solved using CPLEX. Beginning the n -phase, the problem $\text{BMIQP}(n, 0)$ is solved for each $n = \{1..|\mathcal{N}_+\}$ and the values of $\sigma(n, 0)$ are plotted to select n^* . Having found a value for n^* , the e -phase is performed. The problem $\text{BMIQP}(n^*, K)$ is solved for increasing values of K until the stopping criteria. At each step, the integer solution, $y^*(n^*, K)$ is recorded before adding it to the set of cuts. The remainder of this section shows the results of this approach on each of the five examples.

Single Injection Examples

In the first example, we simulate an injection from node 435. Formulating and solving the OCQP, we get the solution shown in Figure 4. Here, we see two dominant nodes, 2301, and 435. There are some smaller injections from other nodes, but with the solution of the OCQP alone, it is not known if these injection profiles have a significant effect on the least squares objective. Partitioning the elements of m gives us 7 nodes to consider in $\text{BMIQP}(n, 0)$ and a total of 70 elements in m_+ . In the n -phase, we record the $\sigma(n, 0)$ values shown in Figure 5. The abscissa shows the value of n in $\text{BMIQP}(n, 0)$ and the ordinate shows the corresponding value of $\sigma(n, 0)$. Here, we clearly see at $n=1$ that a single injection is capable of a very good match with the observed data. Executing the e -phase with $n^*=1$, we record the $y^*(n^*, K)$ values shown in Table 2. This table summarizes the results by listing the number of cuts, K in the first column, the value for $\sigma(n^*, K)$ in the second column, and elements of $y^*(n^*, K)$ that were 1 (i.e. the nodes represented in the solution). Here, the e -phase identifies the two possible injection locations as node 435 or node 2301. Overall, these results tell us that a single injection location is likely, and that its location is either 435 or 2301. We now know that nodes 430, 431, 2401, 2501, and 2601 do not have a significant effect on the least squares objective.

The OCQP solution for a single injection from node 801 is shown in Figure 6. Here, we have only two injection locations present, nodes 801, and 802. We may have a scenario with a single injection location and that injection is from either node 801 or 802. Or,

we may also have a double injection scenario involving both nodes. In this example, if we look at the network diagram shown in Figure 3 we can see that nodes 801 and 802 are neighboring nodes and we would conclude that we likely have a single injection scenario from either node 801 or node 802. When formulating problem BMIQP, we have only 2 nodes to consider and 27 elements in m_+ . The results of the *n-phase* are shown in Figure 7. Again, we clearly see that a single injection is capable of producing the observed data. The *e-phase* results, in Table 3, show that a single injection from node 801 is capable of matching the data, as is a single injection from node 802. Due to the sparsity of the sensor network, and the flow patterns, these two locations are indistinguishable.

Multiple Injection Examples

In the third example, we simultaneously inject contaminant from nodes 435 and 51. We see in the solution of the OCQP, shown in Figure 8, that there is increased non-uniqueness and model error and the OCQP identifies many possible injection locations. Performing the two-phase approach, we have 14 nodes to consider and 164 elements in m_+ . The *n-phase* results are shown in Figure 9. Here, a single injection, on its own, is not capable of matching the observed data, however, a solution with two injection locations is able to match the data well. The *e-phase*, with $n^*=2$, finds the solutions given in Table 4. As viable injection scenarios, we see every combination of 435 or 2301 with every combination of 51, 71, or 70. The *e-phase* results from this example agree with the first example, that injections from nodes 435 and 2301 are indistinguishable. Furthermore, we see that injections from 51, 71, and 70 are indistinguishable. This solution shows us that we have two injections occurring in the network, one of them is from node 435 or node 2301, and one is from node 51, 71, or 70. The two-phase approach is capable of separating the non-uniqueness associated with each region. Furthermore, it has removed, from the OCQP solution, the nodes that do not largely contribute to the least squares objective.

In the fourth example, we test simultaneous injections from nodes 435 and 801. The

solution of the OCQP is shown in Figure 10. Partitioning m , we have 7 nodes to consider and 90 elements in m_+ . The n -phase results, given in Figure 11, tells us that we should consider two locations. We know from previous examples that nodes 435 and 2301 are indistinguishable from each other and that nodes 801 and 802 are indistinguishable from each other. Therefore, we would expect e -phase results that show every combination of 435 or 2301 with every combination of 801 or 802, which is exactly the result that we see in Table 5.

In the final example, we test the two-phase approach with simultaneous injections from nodes 435, 801, and 51. The solution of the OCQP is shown in Figure 12. It would be very difficult to determine the distinct injection possibilities from the OCQP solution alone. Partitioning m , we have a total of 14 nodes to consider and 181 elements in m_+ . We see in the n -phase results, shown in Figure 13, that neither $n=1$ or $n=2$ are able to match the observed data. The results of the n -phase indicate that there are likely 3 injection locations involved. Setting $n^*=3$, the e -phase results are shown in Table . This shows the possible injection scenarios as any combination of nodes 435 or 2301, with any combination of nodes 51, 70, or 71, with any combination of nodes 801 or 802, consistent with the indistinguishable nodes from the examples above. The two-phase approach is able to distinguish that there are three injection locations and provide distinct injection scenarios that include the true injection locations.

Conclusions and Future Work

The results demonstrate that the base mixed integer quadratic programming formulation can separate out nodes from the OCQP that do not dramatically contribute to the least squares objective. The greatest strength of this two-phase approach is its ability to identify the number of likely injection locations and then systematically search for the distinct injection scenarios.

These tests were performed on an Intel 2.4 GHz Xeon Processor machine. For all examples, the execution time for the n -phase and the e -phase was reasonable for use in a real-time setting. The longest e -phase execution time was less than 15 seconds. These

fast solution times in the *e-phase* are only possible because of the problem reduction procedure. Further computational tests could compare the cost of solving the full problem against the combined cost of generating the reduced problem and then solving the reduced problem to determine when each technique is appropriate.

This approach is subject to problems of scale, however. The *n-phase* relies on differences in the value of the least squares objective to determine the likely number of injections. Consider the case with one large continuous injection that has a huge effect on the least squares objective, and one small continuous injection that has a minor effect on the least squares objective. It is possible for us to mistake the tiny difference between $\sigma(1, 0)$ and $\sigma(2, 0)$ as noise or model error and incorrectly determine that the number of injections is one. We do not feel that this is a huge drawback since the larger injection would have a much more dramatic effect on contaminant levels in the network and it is likely we would want to first investigate this injection location anyway. Once that injection has been stopped or flushed its way through the system, the second, smaller injection would then be realized. If the two contaminant regions are separated, a windowing approach like that described in previous work (Laird et al., 2004) could also be used to solve each problem independently and would not be subject to the issues of scaling.

The formulation used in this paper makes the same assumptions as in previous work (Laird et al., 2005, 2004; van Bloemen Waanders et al., 2003). Namely that the sensors can provide some linear measure of the degree of contamination and that the real-time network flows are known. Future work will address both of these issues. First, the problem can be reformulated to allow for sensors that cannot provide a measure of the degree of contamination, but only indicate the presence or lack of contaminant. The solution to this reformulated problem will, of course, be less precise and it is likely that the number of possible scenarios requiring investigation will increase. Furthermore, in a real life situation, the network water demands will only be loosely characterized. We propose to consider the uncertainty associated with these parameters through the use of a multi-scenario framework. Here, a single optimization problem is formulated with a large number of scenarios, each being a statistical sample from the expected demand

distributions. This approach has been previously described for the design of chemical plants under uncertain conditions in Rooney and Biegler (2003) and decomposition approaches exist to solve this large problem efficiently. We believe that these are the next critical steps necessary to solve the problem of effective source inversion in drinking water networks.

Acknowledgments

The authors would like to acknowledge Dr. F. Shang whose conversation renewed our interest in this problem. This discussion encouraged us to reconsider problem reduction techniques, allowing the development of the work within this paper.

References

- Berry, J., Fleischer, L., Hart, W. and Phillips, C. (2003), ‘Sensor placement in municipal water networks’, *Proceedings of the EWRI Conference, Philadelphia* .
- Biegler, L. T., Grossmann, I. E. and Westerberg, A. W. (1997), *Systematic Methods of Chemical Process Design*, Prentice Hall International Series in the Physical and Chemical Engineering Sciences, Prentice Hall PTR, Upper Saddle River, New Jersey 07458.
- Fourer, R., Gay, D. M. and Kernighan, B. W. (1993), *AMPL: A Modeling Language for Mathematical Programming*, The Scientific Press (now an imprint of Boyd & Fraser Publishing Co.), Danvers, MA, USA.
- Laird, C., Biegler, L., van Bloemen Waanders, B. and Bartlett, R. (2005), ‘Contamination source determination for water networks’, *A.S.C.E. Journal of Water Resources Planning and Management* .
- Laird, C. D., Biegler, L. T. and van Bloemen Waanders, B. (2004), ‘Real-time, large scale optimization of water network systems using a subdomain approach’, *submitted for publication, presented at Second CSRI Conference on PDE-Constrained Optimization, Santa Fe, NM* .
- Ostfeld, A. and Salomons, E. (2003), ‘An early warning detection system (ewds) for drinking water distribution systems security’, *Proceedings of the EWRI Conference, Philadelphia* .
- Presidential Decision Directive, P. W. J. C. (n.d.), *Critical Infrastructure Protection: Sector Coordinators, Presidential Decision Directive 63*, Federal Register 63, no. 150 (5 August 1998): 41804.

- Rooney, W. C. and Biegler, L. T. (2003), ‘Optimal process design with model parameter uncertainty and process variability’, *AIChE Journal* **49**(2), 438.
- Rossman, L. (2000), *Epanet 2*, Technical report, EPA.
- Rossman, L. and Boulos, P. (1996), ‘Numerical methods for modeling water quality in distribution systems: A comparison’, *Journal of Water Resources PLanning and Management* **122**(2), 137–146.
- Shang, F., Uber, J. and Polycarpou, M. (2002), ‘A particle backtracking algorithm for water distribution systems analysis’, *A.S.C.E. Journal of Environmental Eng* **128**(5), 441–450.
- van Bloemen Waanders, B. G., Bartlett, R. A., Biegler, L. T. and Laird, C. D. (2003), ‘Nonlinear programming strategies for source detection of municipal water networks’, *Presented at EWRI Conference, Philadelphia* .
- Zierolf, M., Polycarpou, M. and Uber, J. (1998), Development and auto-calibration of an input-output model of chlorine transport in drinking water distribution systems., *in* ‘I.E.E.E. Trans. on Control Systems Technology’, Vol. 6(4), pp. 543–553.

Solution No.	Objective Value	n	y_8	y_{12}	y_{13}
1	0.00	1	0	0	1
2	0.00	2	1	1	0
3	0.00	3	1	1	1
4	36.8	2	0	1	1
5	36.8	2	1	0	1
6	191	1	1	0	0
7	191	1	0	1	0
8	449	0	0	0	0

Table 1: Enumerated Solutions to Grid Network Example.

K	$\sigma(n^*, K)$	Nodes Found
0	0.96	435
1	0.88	2301
2	0.12	2401

Table 2: *e-phase* results for a single injection from node 435. The dashed line indicates the cutoff point for the *e-phase* search.

K	$\sigma(n^*, K)$	Nodes Found
0	1.0	802
1	1.0	801
2	—	problem infeasible

Table 3: *e-phase* results for a single injection from node 801. The dashed line indicates the cutoff point for the *e-phase* search.

K	$\sigma(n^*, K)$	Nodes Found
0	0.94	435, 51
1	0.92	435, 71
2	0.92	435, 70
3	0.90	2301, 51
4	0.88	2301, 71
5	0.88	2301, 70
6	0.56	431, 51

Table 4: *e-phase* results for simultaneous injections from nodes 435 and 51. The dashed line indicates the cutoff point for the *e-phase* search.

K	$\sigma(n^*, K)$	Nodes Found
0	0.98	435, 802
1	0.98	435, 801
2	0.94	2301, 802
3	0.93	2301, 801
4	0.56	2301, 2501

Table 5: *e-phase* results for simultaneous injections from nodes 435 and 801. The dashed line indicates the cutoff point for the *e-phase* search.

K	$\sigma(n^*, K)$	Nodes Found
0	0.96	435, 51, 802
1	0.95	435, 51, 801
2	0.94	435, 71, 802
3	0.94	435, 70, 802
4	0.93	435, 71, 801
5	0.93	435, 70, 801
6	0.93	2301, 51, 802
7	0.92	2301, 51, 801
8	0.92	2301, 71, 802
9	0.91	2301, 70, 802
10	0.91	2301, 71, 801
11	0.90	2301, 70, 801
12	0.73	435, 55, 71

Table 6: *e-phase* results for simultaneous injections from nodes 435 , 801, and 51. The dashed line indicates the cutoff point for the *e-phase* search.

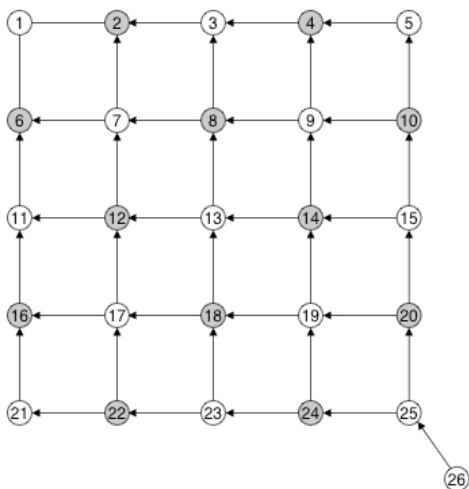


Figure 1: Grid Network Example. A small symmetric grid network with sensors installed at every second node, indicated by the shading.

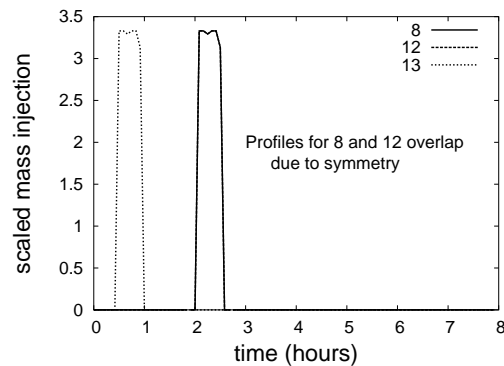


Figure 2: Grid Network Example Solution. Solution of problem (1-4) on the grid network with an injection from node 13 at $t=0.5$ hours.



Figure 3: Municipal Network Model: Diagram of the network model. Contaminant was injected from nodes 435, 801, and 51 as shown in the expanded regions. The locations of the network nodes have been morphed from the true model, but the connectivity remains true.

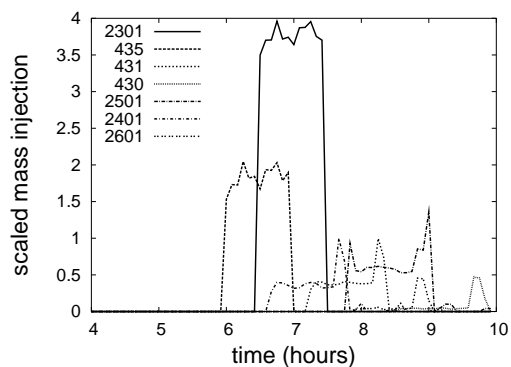


Figure 4: OCQP Solution for a single injection from node 435.

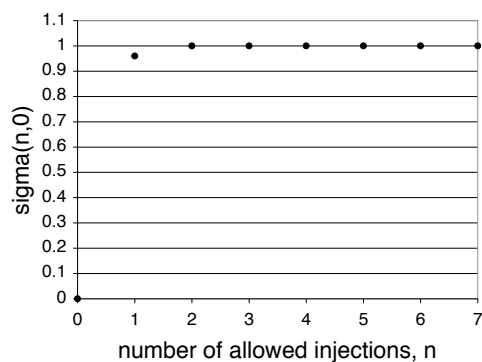


Figure 5: n -phase results for a single injection from node 435.

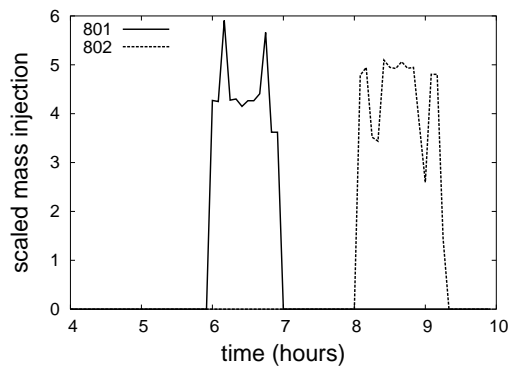


Figure 6: OCQP Solution for a single injection from node 801.

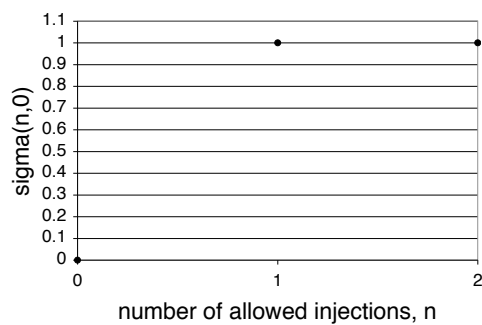


Figure 7: The n -phase results for a single injection from node 801.

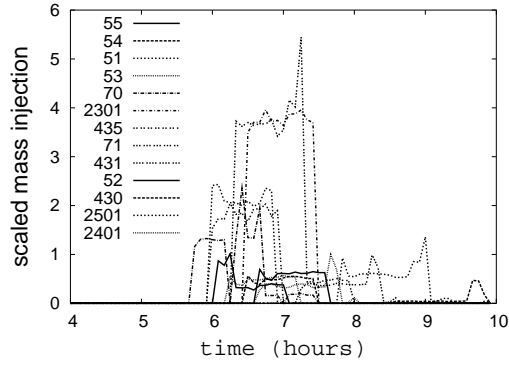


Figure 8: OCQP Solution for simultaneous injections from nodes 435 and 51.

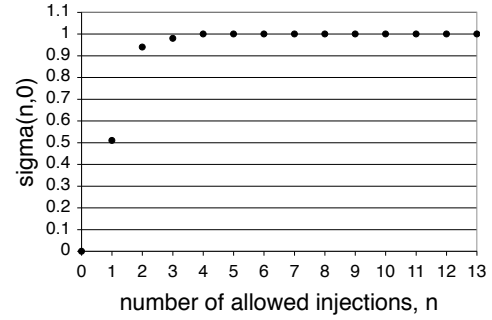


Figure 9: The n -phase results for a double injection from nodes 435 and 51.

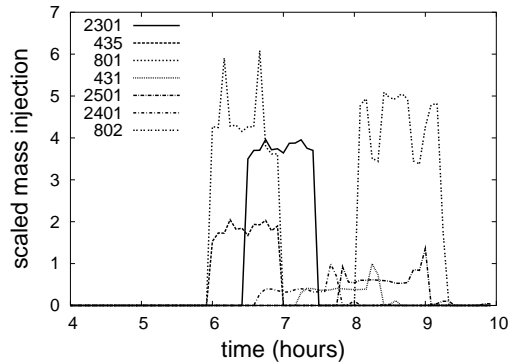


Figure 10: OCQP Solution for simultaneous injections from nodes 435 and 801. The dashed line indicates the cutoff point for the e -phase search.

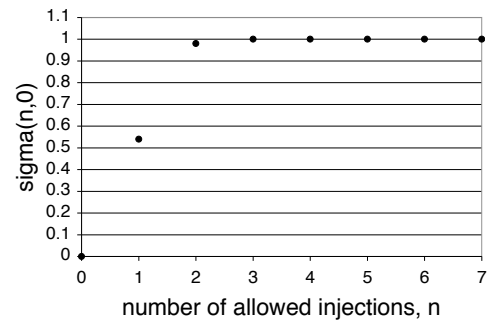


Figure 11: The n -phase results for simultaneous injections from nodes 435 and 801. The dashed line indicates the cutoff point for the e -phase search.

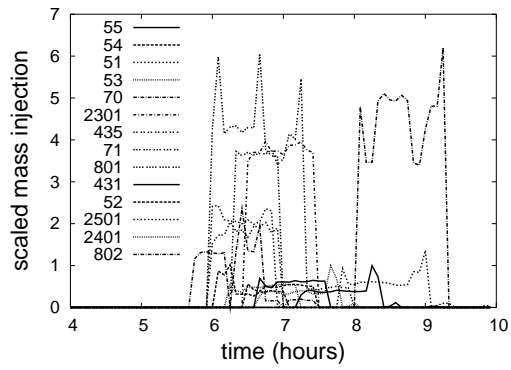


Figure 12: OCQP Solution for simultaneous injections from nodes 435, 801, and 51.

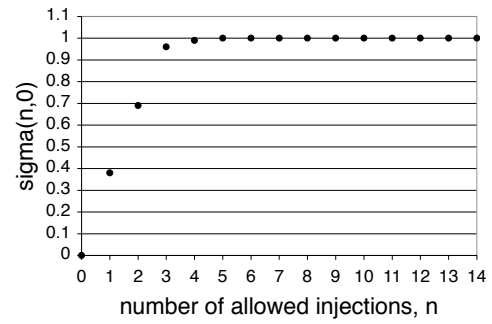


Figure 13: The n -phase results for simultaneous injections from nodes 435, 801, and 51.